EARTHQUAKE ENGINEERING AND STRUCTURAL DYNAMICS
Earthquake Engng. Struct. Dyn. **28**, 109–126 (1999)

FIELD TEST OF AN INTELLIGENT STIFFENER FOR BRIDGES AT THE I-35 WALNUT CREEK BRIDGE

WILLIAM NEFF PATTEN*,†, JINGHUI SUN‡, GUANGJUN LI,‡ JEFF KUEHN‡ AND GANG SONG‡
Center for Structural Control, The University of Oklahoma, 865 Asp Avenue, Room 212, Norman, OK 73019, U.S.A.

SUMMARY

The addition of controllable hardware to structures to mitigate vibration that results from dynamic loads is an emerging area of technological development. The paper describes the results of a research project that was conducted to test a relatively new approach to structural control: an adjustable semi-active hydraulic actuation system that was attached to an in service interstate bridge. The system, which is powered by a 12-volt automative battery, has been tested over a 2- year period. Data indicates that the system reduces truck induced peak stresses by over 50 per cent, and calculations, per NCHRP 299, indicate that the safe life of the structure is increased by approximately 50 yr. The installed cost of the system represents less than 10 per cent of the cost to replace the bridge. Copyright © 1999 John Wiley & Sons, Ltd.

KEY WORDS: intelligent stiffener; semi-active control; vibration; bridge; safe life; hydraulic

INTRODUCTION

There is an evident need to develop technologies that can extend the useful life of bridges. A recent report to the US congress by the federal highway administration indicates that approximately 25 per cent of the bridges in the US are rated as deficient. It is estimated that it will require an investment of 7 billion dollars per year for the next 26 yr to rebuild or replace the bridge infrastructure in the USA. If the bridges are not upgraded, the nation's commerce will suffer predictable declines. The Center for Structural Control (CSC) at the University of Oklahoma has been engaged in a multiyear effort to develop smart technologies that can be relied on to extend the useful service life of bridges. The research effort has culminated in the development of an Intelligent Stiffener for Bridges (ISB) that can be retrofitted to an existing bridge. This paper reports the first successful demonstration of the ISB technology on an in-service bridge. The results indicate that the ISB system can add decades of service life to an existing bridge.

* Correspondence to: William Neff Patten, Center for Structural Control, The University of Oklahoma, 865 Asp Avenue, Room 212, Norman, Oklahoma 73019, U.S.A. E-mail: CSC@ou.edu
† Ph.D., P.E.
‡ Ph.D.

Contract/grant sponsor: U.S. Federal Highway Administration; Contract/grant number: NCHRP #2125

CCC 0098–8847/99/020109–18$17·50

Received 3 March 1998

The ISB consists of an otherwise generic stiffener retrofitted to a bridge. The stiffener is unique in that it is equipped with an adjustable hydraulic link that is used to regulate the amount of stiffness (and damping) that is provided by the stiffener as vehicles pass over the bridge. The ISB acts much like a muscle, sometimes flexing, and other times remaining relaxed. A logic is presented that results in an effective control of the ISB. The ISB is referred to as a semi-active control system because it uses no line power or pumps.[1–2] It is energized by a 12-volt automobile battery. This paper describes the design features of the ISB and the test bridge on which the ISB was mounted. The steps used to establish a reduced order FEM of the bridge are recounted. The paper also provides a brief description of the procedure used to validate the bridge model. The performance of the installed ISB system is assessed via experimental results.

THE WALNUT CREEK BRIDGE

The test site is located on Interstate 35 in the vicinity of Purcell, Oklahoma. I-35 has been designated as an international corridor. It originates at the Mexican border (at Loredo, TX) and terminates at the Canadian border (at Duluth, MN). The study was restricted to the particular bridge that carries the north bound two lanes of traffic. An identical two-lane bridge at the site carries the southbound traffic. The bridge was originally constructed in 1971 and was opened to traffic in 1972. Periodic traffic counts indicate that the northbound bridge carries just over 18,000 vehicles per day, including approximately 3100 heavy trucks. The largest number of trucks are typically 5-axle, 12·8 m tractor-trailers. One unusual feature of the truck traffic at the test bridge is the passage of trucks laden with rock. A quarry, which is located south of the site supplies much of the gravel used in the Oklahoma City area. The trucks that carry rock are typically configured with 5 axles with a 9·8 m wheel base, weighing 36,320 kg. There are also a large number of dump trucks, which are configured with a steering axle and a tandem axle, and a 4·3 m wheel base. Those vehicles are permitted at 25,880 kg.

The site was selected because the bridge superstructure exhibited visually detectable deflections when trucks pass over. The bridge was also selected because it was closer (40 km) to the University of Oklahoma (OU) campus than any of the other candidate bridges considered. The superstructure consists of five continuous girders weighing 196·5 kg/m, with a 1·37 m deep web and 0·36 m wide flanges. The reinforced concrete deck is 0·19 m thick. The bridge, which has a skew of 45°, is supported by three intermediate concrete piers at 30·5 m intervals. The superstructure includes disphragms constructed of lightweight elements located at 6·1 m intervals along the span. Figure 1 depicts a cross section of the superstructure. Once the bridge was selected then the blue prints were used to develop a Finite Element Model (FEM) of the entire structure.

The I-DEAS® FEM software (by Structural Dynamics Research Corporation) was selected for the analysis. I-DEAS has a state-of-the-art graphics support module, which makes it especially easy to illustrate the system. The FEM consisted of 410 thin shell elements, 620 beam elements (including 'I', 'T', and angle), 316 rigid bars and 74 solid elements. The base model included 811 nodes, requiring 4800 coupled equations of motion. Boundary conditions at the support piers were included in a routine manner.

In order to validate the model, modal testing of the bridge was conducted. That work began with the placement on the bridge superstructure of a densely packed system of sensors that were installed to record the response of the bridge to ambient (truck) loads as well as a modal excitation loads. A systems of 36 Piezo-resistive accelerometers were installed at the locations

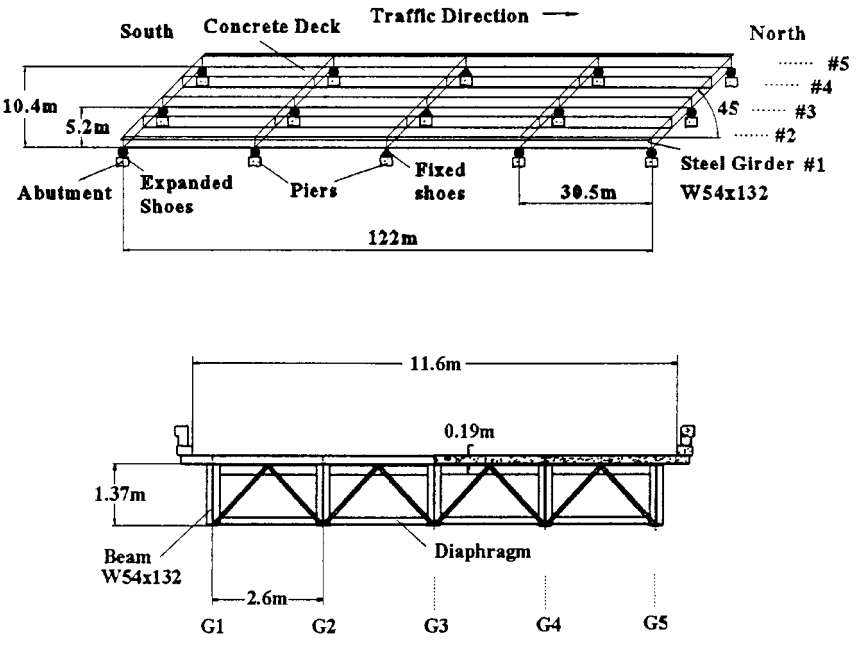

Figure 1. Superstructure of the Walnut Creek bridge

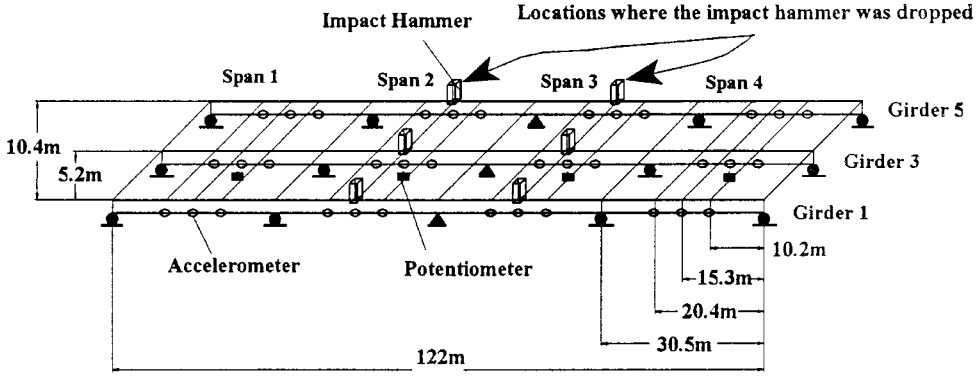

Figure 2. Modal test system set-up at the Walnut Creek bridge

shown in Figure 2. All accelerometers were rated for 2*g* output. In addition, the center point of each span was outfitted with a string potentiometer, which was used to measure the absolute displacement of the superstructure. Also installed were strain gauges to measure the strain at the centre of each of the girders at the bottom flange. Additional strain gauges were also installed to establish the neutral axis of each of the girders.

The long distance from sensors to the data acquisition system (as much as 180 m) made it impossible to achieve the goals of this project with conventional signal conditioning technology. Instead, the research team developed and installed a low-cost voltage to frequency and frequency to voltage modulation/demodulation system to convey sensor data to the central processor.

In order to verify the analytical model, experiments were conducted. A drop hammer was constructed, with an instrumented 160 kg head which, when released, would fall free 1·9 m, creating an impulsive force of 11,350 kg. The hammer was dropped four times at six different locations and the output of the 36 accelerometers was recorded. The test data was then used to extract modal frequencies and mode shapes.

Table I lists the first 4 modal values obtained via experiment and simulation. The damping associated with each of the modes is also shown. Figure 3 depicts various mode shapes. Figure 4 depicts two transfer functions obtained from the tests. The two transfer functions represent the ratio of the output acceleration to the input (impulse) force. The two accelerometers were mounted on the opposing sides of the bridge in the same span, at the middle of the span. A comparison of the two transfer functions makes it clear which mode is purely bending, which is purely torsion, and which mode represents a combination of bending and torsion. A related paper describes the particulars of the modal testing analysis.[3] That reference includes an assessment of the accuracy of the mode shapes obtained via the modal assurance criterion. It suffices to note that the modal frequencies and mode shapes predicted by the corrected FEM are a close fit to those measured in the field. Once the FEM was established, then steps were taken to verify the model in the time domain. Simulations of the dynamic response of the bridge were conducted using a reduced order model (ROM) of the bridge. A coarse mesh of the structure was established that produced a 225 degree of freedom ROM. The Guyan IRS method[4,5] was used to adjust differences between the full FEM and the ROM. Table II lists a comparison of the first 10 mode shapes of the full FEM and the ROM. The work also established the concurrence of the mode shapes, for the full FEM and ROM.

Table I. Modal frequencies and modal damping of the Walnut Creek bridge, test vs. simulation

Mode order	Test (Hz)	FEM (Hz)	Test damping
1	2·54	2·52	0·024
2	3·01	2·95	0·014
3	3·25	3·28	0·016
4	3·63	3·62	0·018
5	3·88	3·90	0·014
6	4·25	4·34	0·014
7	4·56	4·48	0·022
8	4·78	4·67	0·025
9	5·01	4·93	0·028
10	5·23	5·52	0·021
11	7·47	7·70	0·025
12	7·78	7·82	0·031
13	8·18	8·30	—
14	10·1	10·4	—

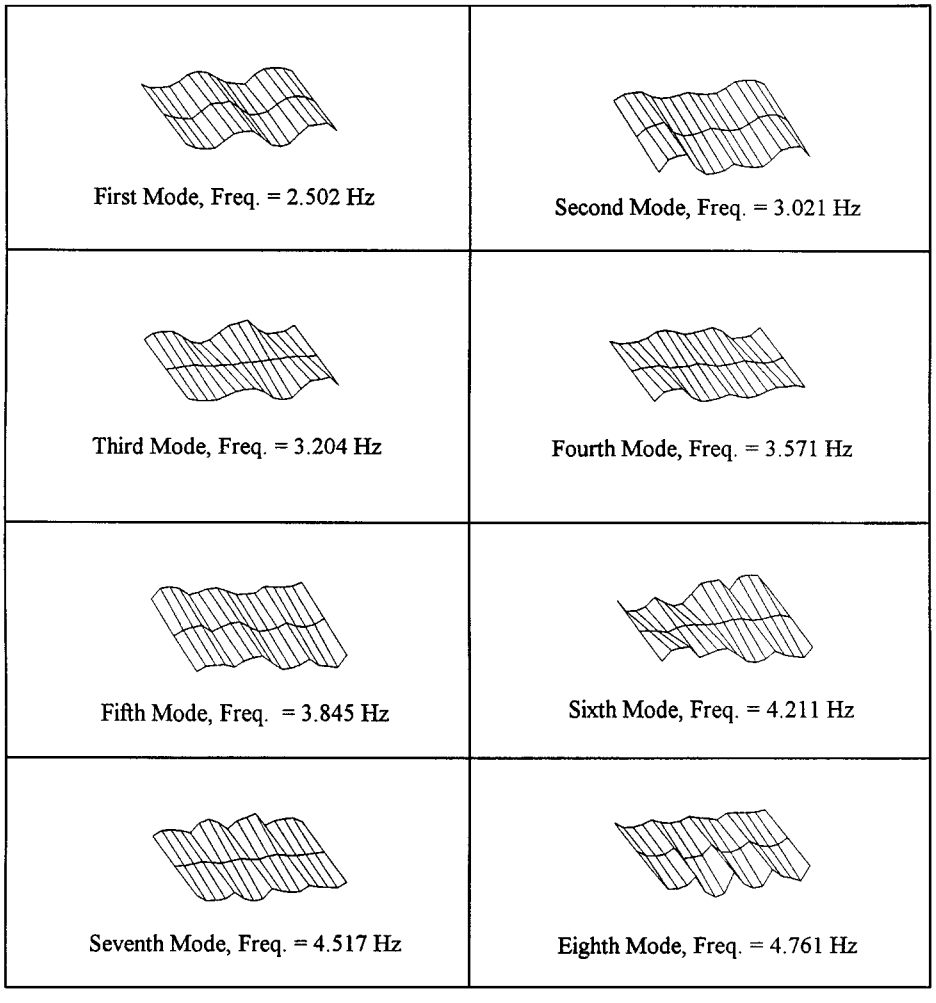

Figure 3. Test mode shapes of the Walnut Creek bridge superstructure

The CSC team also developed a model of the chassis dynamics of a test truck (Figure 5). A 5-axle tractor-trailer dump truck (which is referred to as the Rock Truck (RT)) with a 10·4 m wheel base was employed (the rear tandems act as a single unit for heave motion). Tests were conducted to validate the truck dynamic model. The mass and compliance of the test truck are listed in Table III. Prior to conducting simulations of the bridge/truck system the profile of the road at the entrance to the bridge was measured (see Figure 6). The simulation versus the measured response of the bridge at the bottom flange of the centre of the girder #3; when the RT passed over the bridge in the right lane at 88 km/h is shown in Figure 7. The close correspondence between the measured and simulated response exhibited by this and several other tests made it clear that the ROM of the bridge provides a high fidelity replication of the bridge dynamic response.

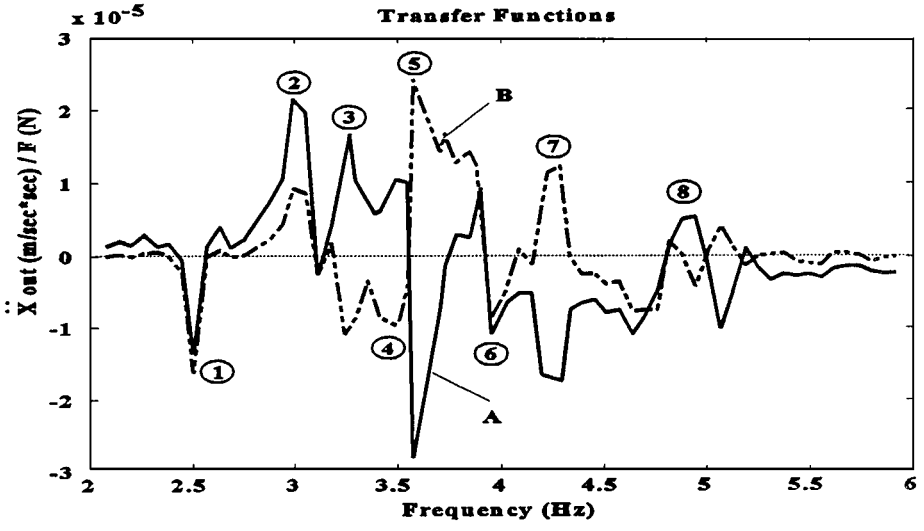

Figure 4. Transfer functions obtained from the modal test; A = girder #1, B = girder #5, at the middle of span #1; mode numbers are shown circled (F = impact force)

Table II. Comparison of bridge test modes with ROM modes

Mode	Frequency (Hz) full FE model	Frequency (Hz) Guyan IRS ROM
1	2·52	2·53
2	2·95	2·96
3	3·28	3·30
4	3·62	3·63
5	3·90	3·93
6	4·34	4·35
7	4·48	4·50
8	4·67	4·70
9	4·93	5·02
10	5·52	5·55

DESIGN OF A CONTROL SYSTEM

Once a reliable model of the bridge had been identified, then the CSC team began the control system design. The first step in that process included an extensive analysis of test data collected during the passage of large trucks across the bridge. A wide variety of truck types, and traffic density patterns were included in the examination. Figure 8 depicts the frequency response of one bridge accelerometer as a typical tractor-trailer moved across the bridge. The study made it clear that various combinations of modal participation occurs, depending on the type of trucks, their

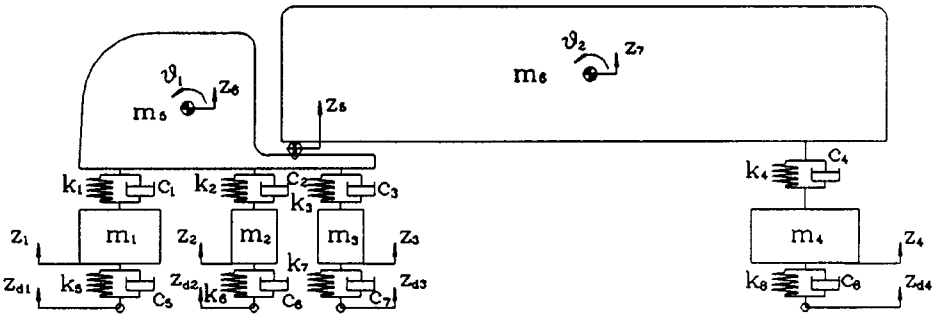

Figure 5. Rock truck (36,320 kg) dynamic model

Table III. Test truck chassis parameters

Symbols	Unit	Value	Symbols	Unit	Value
m_1	kg	250	k_6	N/m	1·58e + 6
m_2	kg	544	k_7	N/m	1·58e + 6
m_3	kg	500	k_8	N/m	3·15e + 6
m_4	kg	794	c_1	N/s/m	6·13e + 3
J_{G6}	kg m^2	5·26e + 3	c_2	N/s/m	8·75e + 3
J_{G6}	kg m^2	6·3e + 4	c_2	N/s/m	8·75e + 3
k_1	N/m	2·63e + 5	c_4	N/s/m	1·75e + 4
k_2	N/m	3·68e + 5	c_5	N/s/m	8·75e + 2
k_3	N/m	3·68e + 5	c_6	N/s/m	1·75e + 3
k_4	N/m	2·36e + 5	c_7	N/s/m	1·75e + 3
k_5	N/m	7·88e + 5	c_8	N/s/m	3·5e + 3

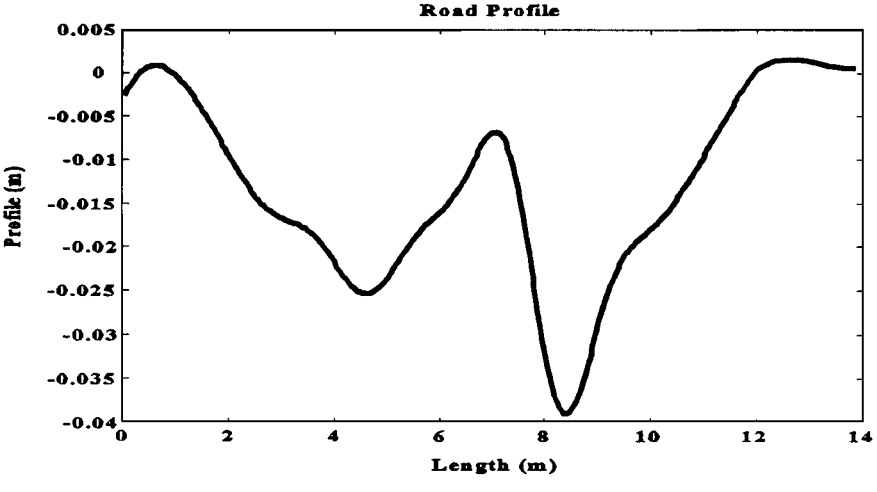

Figure 6. Road profile at the entrance of the Walnut Creek bridge

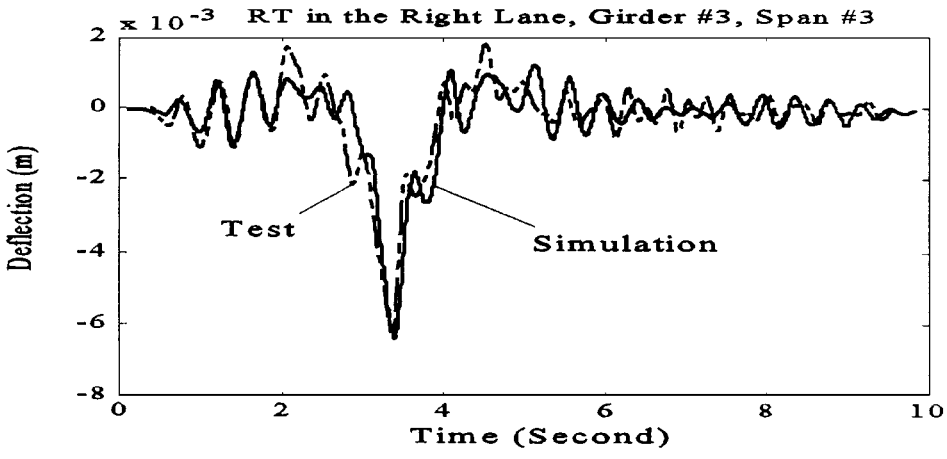

Figure 7. Uncontrolled response of the bridge; simulation vs. test results, rock truck in the right lane at 88 km/h, Girder #3, (Span #3, bottom flange)

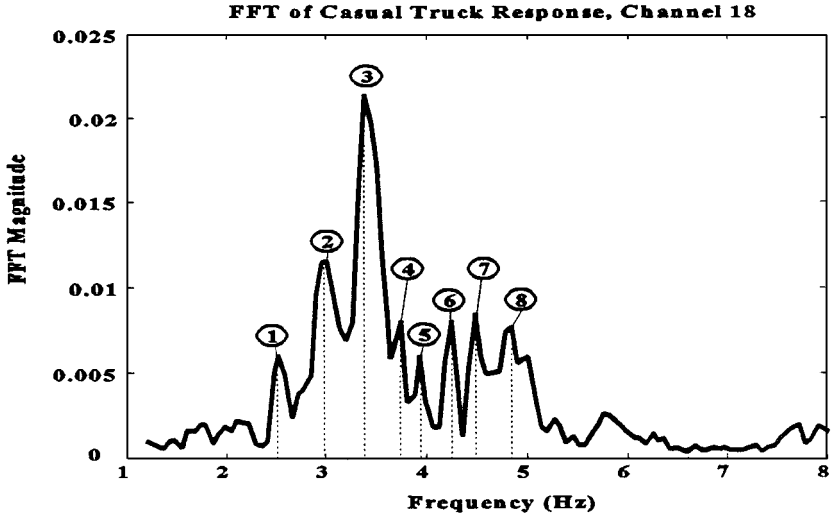

Figure 8. FFT of accelerometer at girder #5 (span #4), in response to the passage by a typical tractor-trailer travelling at 97 km/h; bridge modes are indicated in circles

weights and the traffic pattern. The data also confirmed that the dominant response of the bridge was limited to those modes below 10 Hz. This observation established the required bandwidth of the controller hardware. The measurements were also used to establish an upper bound on the vibratory displacement of the bridge superstructure. In addition, the data made it clear that a very high percentage of the heavy trucks crossing the bridge were coupling dynamically with the bridge. This effect produces dynamic amplitudes that are typically greater than twice the static amplitude (see Figure 9). The static response was obtained by making the same truck travel across

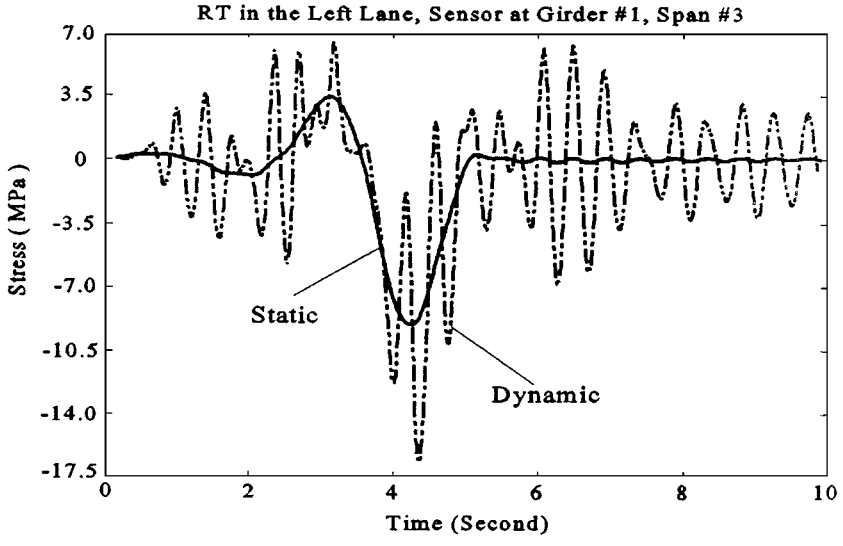

Figure 9. Stress response at the centre of girder #1, (span #3) bottom flange, when the rock truck (36,320 kg) crosses the bridge at 97 km/h

of the bridge at 2 km/h. The coupling is pronounced because of the chassis vibration modes of the truck are similar to the lower fundamental modes of the bridge. A survey by the CSC team of five additional steel girder bridges on I-35 in Oklahoma, with spans ranging from 24·5 to 42·8 m indicates that each of those bridges exhibit similar bridge/truck resonance coupling.

With the knowledge of the frequency and amplitude content of the ambient truck induced loads, the synthesis of a control design was initiated. The design process relied to a large extent of initial decisions such as how to organize the topology and kinematic arrangement of the components. The basic mechanism selected (Figure 10), is similar to the arrangement proposed by Leipholz and his coworkers[6] for the study of an actively controlled truss element.

The closed loop operation of the ISB relies on the physical state of the bridge and of the hydraulic pressure in each of the actuators (Figure 11). This information is used at each point in time to determine whether it is better to open or close a bypass valve on each of the hydraulic actuators. A Lyapunov analysis was used to establish the closed loop control design. An abbreviated description of the analysis that was used to establish a feedback control is given in the appendix. A complete description of that design analysis is offered in a paper that is a companion to this one.[7] The control is fashioned to reduce the maximum displacement and velocity of the girders, which in turn reduces the stress that each of the girders experience during the passage of a truck. In addition, the ISB mechanism is intended to shed loads away from those parts of the girder that have experienced the largest stresses over the service life of the bridge (here, the centre of the girder between the piers, which is where the maximum positive moment is experienced) to parts of the girder that has been subjected to much lower stress loads over the service life of the bridge.

Once the basic kinematic design was established, then a design study was undertaken to determine the best possible mix of specific design parameters. Noting the basic configuration of

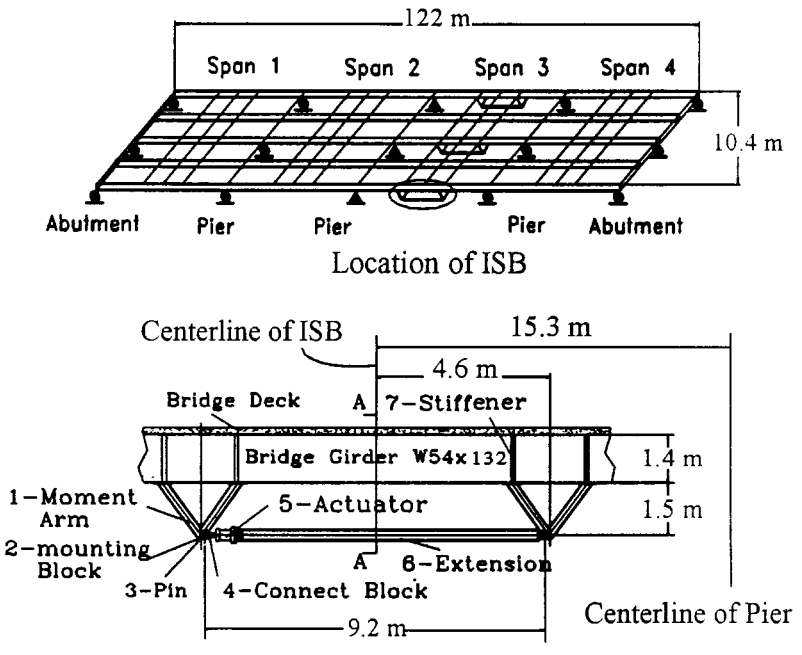

Figure 10. The ISB system set-up in the I-35 Walnut Creek bridge

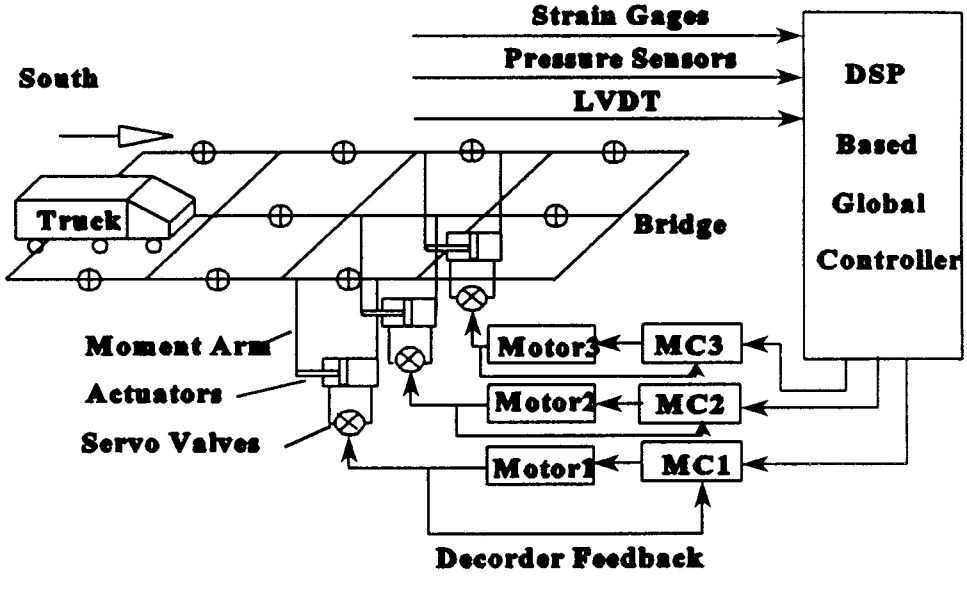

Figure 11. ISB control system layout; MC = micro controller

the ISB, the team used the I-DEAS software and the ROM to determine a feasible design. The selected design reflects a balance between effectiveness and the cost of fabricate, install and maintain the ISB system. The sensitivity of the cost to various kinematics variables, including the distance between the moment arms, the dimensions of the actuator, the location of the ISB relative to the piers, the placement pattern of the ISB, the sizing of the hydraulic plumbing, and the stiffness and weight of the ISB assembly, were each considered. A subsequent analysis was conducted to determine the maintainability of the system, and the extent to which fatigue life would be increased by the ISB system.

INSTALLATION AND TESTING

Subcontracts were awarded for the fabrication of the hydraulic actuators, the extension elements, and the moment arms. The actuators and extension elements were bolted together at the CSC facilities. The installation was accomplished using monorails and a block and tackle system. A temporary raod was installed using fill from the creek bed. The first step in the installation was the drilling of the girder web to attach web stiffeners. Next, holes were carefully drilled in the flange of the girders one girder at a time. The effectiveness of the design relied, in part, on the ability of the ISB system to transmit forces at a specified moment in time. To that end, the installation required considerable care in the location and size of the holes drilled in the flanges. Tapered bolts and reamed holes were used to guarantee a no-slip condition between the girder and the ISB. The moment arms for the ISB assembly were then hoisted into position, and bolted up. Following installation of the moment arms, the actuator/extension assembly was hoisted into place. The process was repeated for each ISB assembly. Traffic was never impeded during the construction effort. The installation of the ISB structural hardware was completed in three weeks. Once the mechanical hardware was installed, then the CSC team installed the micro-controller system. The installed ISB system is shown in Figure 12.

Once the hardware was installed then several tests of the ISB were conducted. A test consisted of making one or more trucks travel over the bridge at either a crawl speed, or at the posted speed limit. Some of those tests truck were instrumented. The first series of tests were conducted to determine the difference in response produced when the ISB actuator valves are locked open. In that mode, the hydraulic actuators function much like a simple passive damper. Figure 13 depicts the stress response of Girder 3 when the 36,320 kg five-axle RT traverses the bridge in the right line at 110 km/h. The first trace (solid line) depicts the response prior to the installation of ISB. The dotted trace indicates the response, with the ISB installed, but with the valve fixed open (passive damper mode). The result indicates that the damper has very little effect on the maximum, strain, but the residual off-peak vibration is reduced by over 50 per cent once the truck has passed over.

The tests also provided a means for iteratively improving the control performance of the system. The controlled response of the bridge with the RT travelling at 105 km/h in the right lane is shown in Figure 14. This response is compared to the response of the bridge under the same conditions, but without the ISB attached. A test with a 54,480 kg six-axle tractor-trailer travelling at 105 km/h in the right lane is shown in Figure 15. In all the cases shown, the effectiveness of the ISB is easily recognized. Figure 16 depicts the time history of the control commands (1 = open, 0 = close) for the 54,480 kg truck test.

Figure 12. The I-35 Walnut Creek bridge with ISB system attached

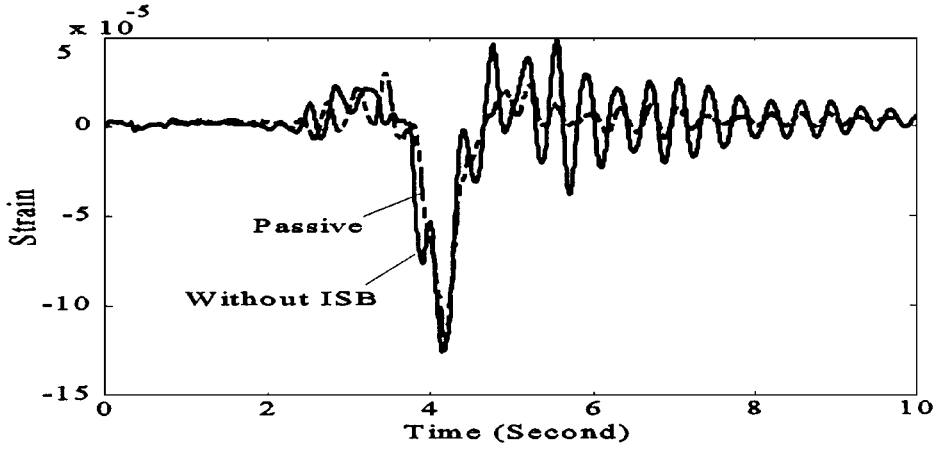

Figure 13. Strain response [at girder #3, (span #3) bottom flange], to the passage by a 36,320 kg Rock truck; (a) when ISB was operated as passive damper, (b) before the ISB system was installed

The primary purpose of the ISB design was to afford a means of extending the remaining useful service life of the test bridge. The ISB accomplishes that goal by reducing the maximum stress range that accompanies the passage of heavy trucks. Figure 17 depicts the maximum stress measured at the centre of the girders when the rock truck crosses the bridge. The stress reduction that accompanies the use of the ISB is significant. The assessment of the effect that the ISB had on

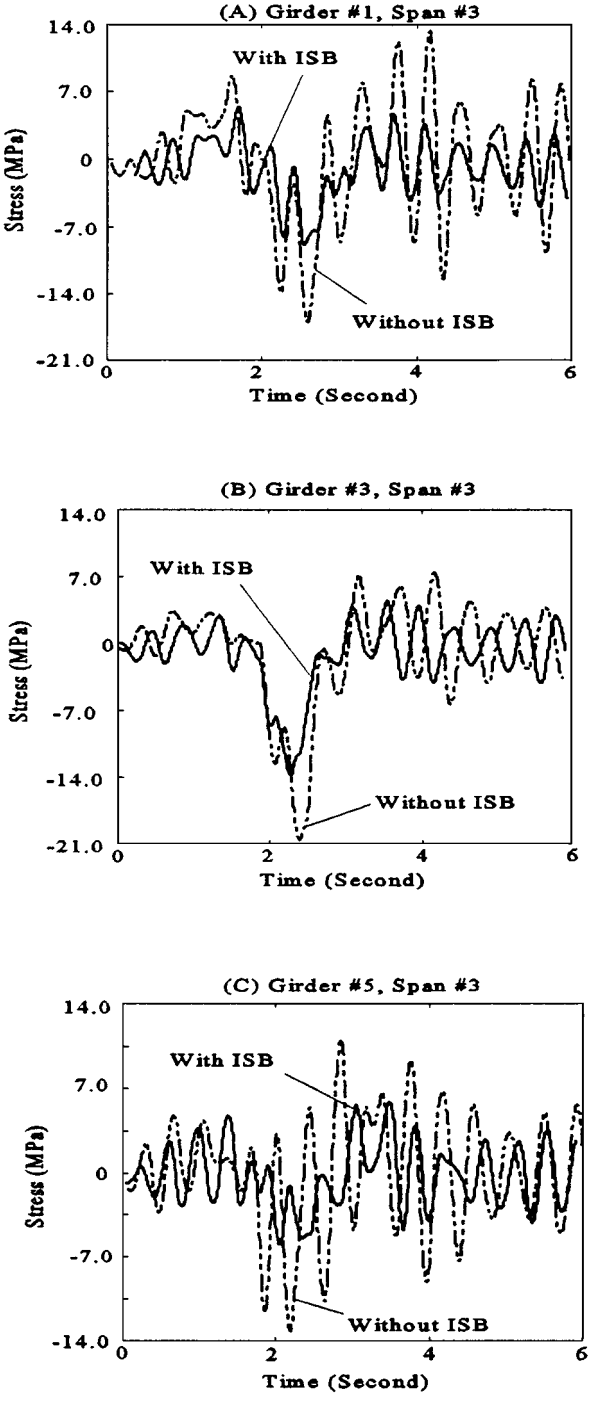

Figure 14. (a), (b) and (c) Closed loop vs. no control performance, with the rock truck travelling in the right lane at 105 km/h

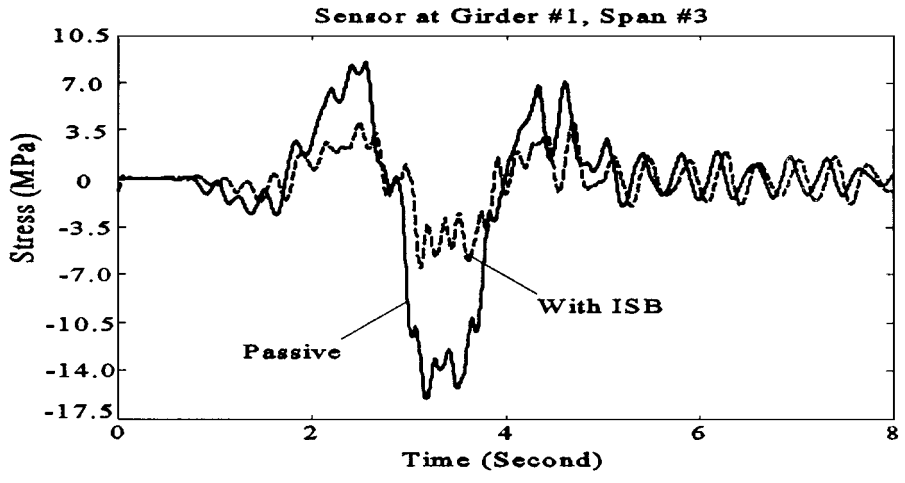

Figure 15. Closed loop control vs. passive (valve open on ISB) performance, when a 120 kip truck passed over the bridge in the right lane at 97 km/h

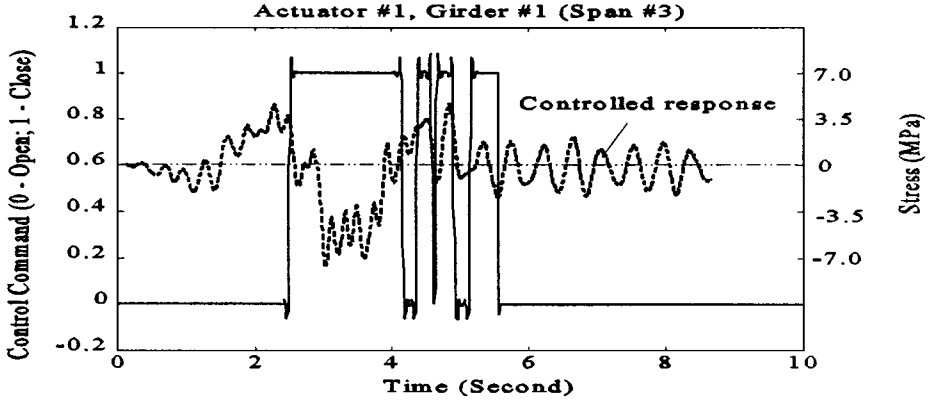

Figure 16. Closed loop control command, 120 kip truck ran over the right lane

the remaining service life of the bridge was conducted by using a specific rule (governing equation) prescribed for that purpose by NCHRP 299.[8] Data was obtained via field measurements with and without control operating. The tests were run several times for various trucks traveling in each lane at the posted speed limit. The calculated differences of remaining safe life when the loaded rock truck crossed the bridge is shown in Table IV for the girders #1, 3 and 5. The minimum addition of safe life produced was 49·6 yr. An almost identical result was observed when the loaded dump truck was employed in the test. The table indicates that prior to the addition of the ISB system, the code indicated negative safe life.

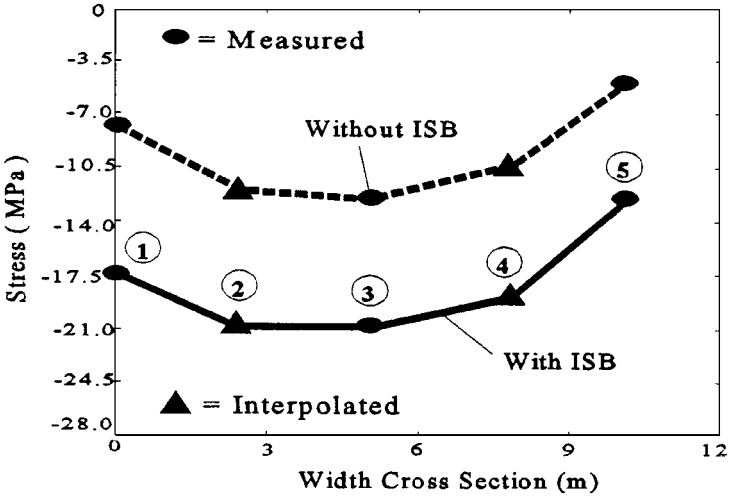

Figure 17. Maximum stress measured at span #3 mid-section, rock truck travelling in the right lane; girder numbers are encircled

Table IV. Remaining safe life (Y_f) of the Walnut Creek bridge based on the rock truck test

	Girder #1	Girder #3	Girder #5
No ISB (yr)	− 12·4	− 13·7	0.40
ISB controlled (yr)	167·7	35·8	110·5
Life extension (yr)	180·1	49·5	110·9

Note:

Safe life (see NCHRP 229): $$Y_f = \frac{f \times K \times 10^6}{T_a \times C \times (R_s \times S_{re})^3} - a$$

$f = 1$, $K = 12$, $R_s = 1{\cdot}35$, $C = 1$ (rainfall count)
$T_a = 3000$ = estimated life time average daily truck volume
$a = 25$ (present age of bridge)
S_{re} = maximum stress range: (1) With ISB = $1{\cdot}54 \times 10^7$ N/m; (2) Without ISB = $3{\cdot}41 \times 10^7$ N/m

CONCLUSIONS

The ISB system was field tested on an in service interstate bridge. The research demonstrated that the device can be designed without having to conduct modal tests; the as-built drawings are sufficient for the seizing of the components. The intelligence required is extremely simple. The on-off control will work with a few as three sensors per actuator; the differential pressure, the stroke of the actuator (sensed in this application via a LVDT mounted on the actuator) and the position of the valve (is the valve open or closed). There is no need to rely on strain guages or

accelerometers mounted on the bridge. This implies that the system can be manufactured and installed without attaching a bridge instrumentation system.

The installed ISB has been tested over the course of 22 months. Its operation is robust to extreme variations in seasonal temperatures. The valve/motor system on each actuator has been demonstrated to be highly reliable. Tests have indicated that the three actuator assembly with the minimal sensor configuration will operate on two 12 V, 1000 amp hour batteries for a minimum of two years. The present system is also equipped with a cellular phone line which is used to monitor the electronics.

Of primary importance is the fact that the ISB operates without a primary power source. The semi-active system cannot pump power into the bridge. This yields the system inherently stable. The system is designed to gracefully degrade to a simple hydraulic damper if semi-active operation is compromised in some manner.

The work demonstrated that the control logic is extremely simple and fail safe, and that the operation of the system can dramatically extend the service life of the bridge (by several decades). The system is also unique in that it only reponds to large loads, thus reducing the amount of stress (over time) that would have been otherwise applied at the points where the ISB connects to the girder. Almost as importantly, the fluid spring effect helps to ensure that the magnitude of the moments produced at the connection points are as much as 30 per cent lower than those moments that would have been produced by a fixed stiffener for the same load. Future work will explore a new design that will make it possible to eliminate the moment arms. This will reduce the possibility of having floating debris damage the ISB.

APPENDIX I. SYSTEM MODEL

A brief overview of the development of the equations of motion of the bridge, and the coupled actuator dynamics are presented here. An extended presentation of this material can be found in Reference 7. The motion equations (FEM) of the Bridge take the following form:

$$M_{\mathrm{b}}\,\ddot{\hat{y}} + C_{\mathrm{b}}\,\dot{\hat{y}} + K_{\mathrm{b}}\,\hat{y} = \Gamma v + \hat{d}(t), \quad \hat{y} \in R^{m} \tag{1}$$

$\hat{y}$ is a vector of global modal unknowns. The matrices, M_{b}, C_{b}, and K_{b}, represent the mass, the proportional damping and the stiffness of the bridge. The first term, on the right-hand side of equation (1), represents the input moments to the girder produced by the ISB assembly. The matrix $\Gamma_{\mathrm{m}\times\mathrm{n}}$ is a Boleean matrix that provides a mapping between the global nodal unknowns and the inputs. The analysis assumes that each control moment is one of a pair with equal magnitudes the opposite sign. The input vector, $\hat{d}(t)$, represents the tire force imposed by the moving vehicle.

An exact model analysis would include the elastic coupling between the bridge and the truck that occurs at the tire/deck interface.[9] The involvement of the truck dynamics in the model will produce a non-autonomous set of system equations which are impractical for control design purposes. In addition, it is not in general possible to measure the dynamics of the vehicle as it crosses the bridge. The analysis here treats the truck tire force as an exogenous disturbance. The dynamics of the ISB system actuator can be characterized by

$$\Delta\dot{P} = -\alpha\beta\,\{A_{\mathrm{p}}\,h\,(\hat{R},\,\hat{y}) + g(\Delta P)\,C_{\mathrm{d}}\,A_{\mathrm{v}}\} \tag{2}$$

The derivation of equation (2) is found in Reference 2. The fundamental observation to be made is that the change in the force (moment) applied is related evidently to changes in the stiffness of the fluid (The first expression on the right-hand side of equation (2)). As well as to the inherent damping associated with the flow across the valve (represented by the second expression on the right-hand side of equation (2)).

The parameter α represents $V_1V_2/(V_1 + V_2)$ where V_1 and V_2 are the respective volumes of each chamber in the two chambered cylinder at any particuar point in time. β is the (pressure dependent) bulk modules A_p is the area of the piston and $h(r, y)$ is a representation of the length change across the ISB actuator, and A_v is the opening (area) at the valve. Nonlinear expression $g(\Delta P)$, has the following form.[10]

$$g(\Delta P) \triangleq \text{sign}\,(\Delta P)\left(\frac{2}{\rho}|\,\Delta P\,|\right)^q \tag{3}$$

C_d is a discharged coefficient (constant) specific to the valve used.

Defining the extended state variable $\hat{x} = \{\hat{y}^T, \dot{\hat{y}}^T, \Delta P\}$, and noting that the applied moment in equation (1) produced by the actuator is defined as $v = h\,A_p\Delta P$, then combining equations (1)–(3) produces the following control model for the bridges/ISB system:

$$\dot{\hat{x}} = A\hat{x} + Bg\,(\Delta P)\,A_v + D \tag{4}$$

where

$$A = \left|\begin{matrix} [0]_{m\times m} & [k]_{m\times m} & [0]_{m\times 3} \\ [-M_b^{-1}\,K_b]_{m\times m} & [-M_b^{-1}\,C_b]_{m\times m} & [hC_d\,A_p M_b^{-1}\Gamma]_{m\times 3} \\ [0]_{3\times m} & [-\alpha A_p\hat{R}]_{3\times m} & [0]_{3\times 3} \end{matrix}\right|_{r\times r} \tag{5}$$

APPENDIX B. CONTROLLER SYNTHESIS

A quadratic Lyapunov function, $\dot{V}$, is first posed;

$$V = \tfrac{1}{2}\,(\hat{x}^T,\, Q\hat{x});\; Q > 0 \tag{6}$$

$$B = \left|\begin{matrix} [0]_{m\times 3} \\ [0]_{m\times 3} \\ -[hA_p]_{m\times 3} \end{matrix}\right|_{2m+3\times 3}, \qquad D = \left|\begin{matrix} [0]_{m\times 1} \\ [\mathrm{d}(t)]_{m\times 1} \\ [0]_{3\times 1} \end{matrix}\right|_{2m+3\times 1}$$

Differentiating $\dot{V}$, then

$$\dot{V} = \hat{x}^T(A^T\,Q + QA)\,\hat{x} + \hat{x}^T Q\,Bg(X)\,C_d\,A_v + \hat{x}\,QD \tag{7}$$

If $\dot{V}$ is negative, then we can conclude that the system is dissipative (stable). It is assumed that a Q exists and that $A^T Q + QA$ can be selected negative semi-definite. The last expression on the right-hand side of the equation (7) is disregarded, because there is nothing that can be done to affect the dissipation of that (disturbance) term. Writing Q as a matrix of column vectors;

$$Q = [\hat{q}_1\;\hat{q}_2,\,\ldots,\hat{q}_r] \tag{8}$$

and noting that the only nonzero entry in B is the last three elements ($b_n = h\,A_p$), then maximum dissipation is assured if A_V (the valve orifice) is selected using the following bi-state control law.

$$\hat{x}^T\,\hat{q}_r,\ \text{sign}\,(\Delta P_r)\begin{cases}\geqslant 0, & A_{vr} = A_{v\min}\\ < 0, & A_{vr} = A_{v\max}\end{cases},\quad r = 1, 2, 3 \tag{9}$$

The vector $\hat{q}_r$ provides a means of weighting the different states to emphasize a particular control objective; here the reduction of the nodal displacement amplitude at the centre of the bridge was the objective of the control action

APPENDIX C. NOMENCLATURE FOR HYDRAULIC

$A_p = 4{\cdot}013 \times 10^{-2}$,	effective piston area of the actuator
$A_{v\max} = 1{\cdot}394 \times 10^{-5}$,	maximum hydraulic orifice area
$A_{v\min} = 0{\cdot}0$,	minimum hydraulic orifice area
$C_d = 0{\cdot}82(0{\cdot}52)$,	service valve fraction coefficient
$\rho = 8{\cdot}83 \times 10^2$,	density of hydraulic damper
$\alpha = 1{\cdot}14 \times 10^{11}$,	coefficient of hydraulic damper
$\beta = 8{\cdot}7 \times 10^7$,	beam element length

REFERENCES

1. G. W. Housner, L. A. Bergman, T. K. Caughey, A. G. Chassiakos, R. O. Claus, S. F. Masri, R. E. Skelton, T. T. Soong, B. F. Spencer and J. T. P. Yao, 'Special issue: structural control: past, present, and future', *J. Engng. Mech.* ASCE **123**(9), 897–971 (1997).
2. W. N. Patten, C. Mo, J. Kuehn and J. Lee, 'A primer on design of semiactive vibration absorbers (SAVA)', *J. Engng. Mech.* ASCE **124**(1), 61–68 (1997).
3. J. Sun, J. Pang, G. Song and W. N. Patten, 'Experimental validation and modal analysis for a highway bridge', *ASME 1997 Design Engineering Technical Conf.*, 14–17 Sept., Sacramento, California, University of Oklahoma, DETC97/VIB-4251, 1997, pp. 1–4.
4. R. J. Guyan, 'Reduction of stiffness and mass matrices', *AIAA J.* **3**(2), 380 (1965).
5. J. O'Callahan, 'A procedure for an improved reduced system (IRS) model', *7th Int. Modal Analysis Conf.*, Las Vegas, Nevada, 17–21 February 1989.
6. M. Abdel-Roman, V. H. Quintin and H. H. Leipholtz, 'Optimal control of civil engineering structures', *J. Engng. Mech. Div. Proc.* ASCE **106**(EM1), 57–73 (1980).
7. W. N. Patten and G. Li, 'Intelligent stress reduction for bridges', in review, *J. Engng. Mech.* (1997).
8. F. Moses, C. G. Schilling and K. S. Raju, 'Fatigue evaluation procedures for steel bridges', *National Cooperative Highway Research Program Report 299*, Transportation Research Board, National Research Council, Washington, DC, ISSN 0077-5614, 1987.
9. W. N. Patten, 'Semiactive vibration absorbers (SAVA) at the I-35 Walnut Creek Bridge', *Final Report*, *No. 2125*, *FHWA*, Oklahoma Department of Transportation, and The University of Oklahoma, OK, 1997.
10. W. N. Patten, R. L. Sack and Q. He, 'A controlled semiactive hydraulic vibration absorber for bridges', *J. Struct. Engng.* ASCE **122**(2), 187–193 (1996).

